

PHENO 2021

LHC LIMITS ON THE B-ANOMALIES MOTIVATED U_1 LEPTOQUARK MODELS

SUBHADIP MITRA (IIIT HYDERABAD)

May 25, 2021

In collaboration with Arvind Bhaskar, Diganta Das, Tanumoy Mandal, & Cyrin Neeraj

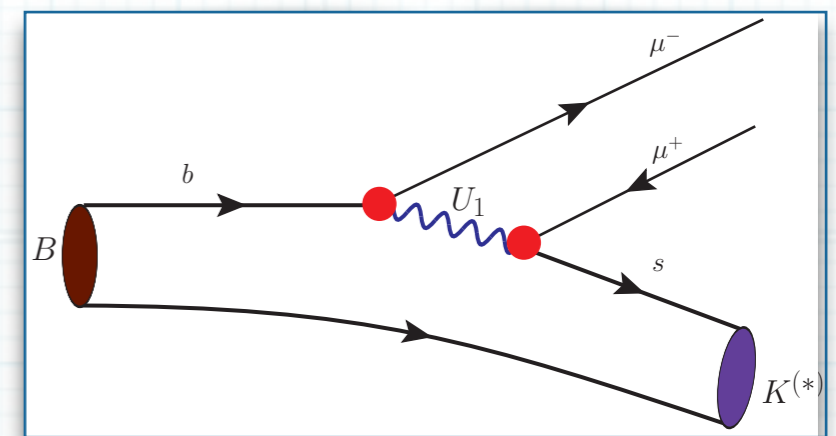
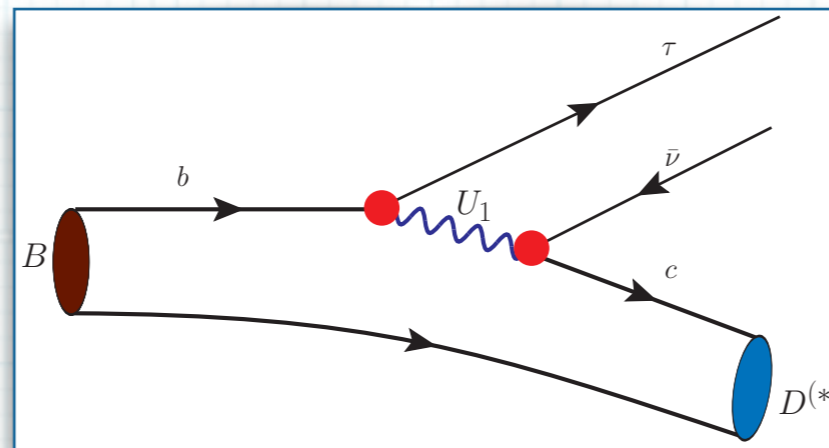
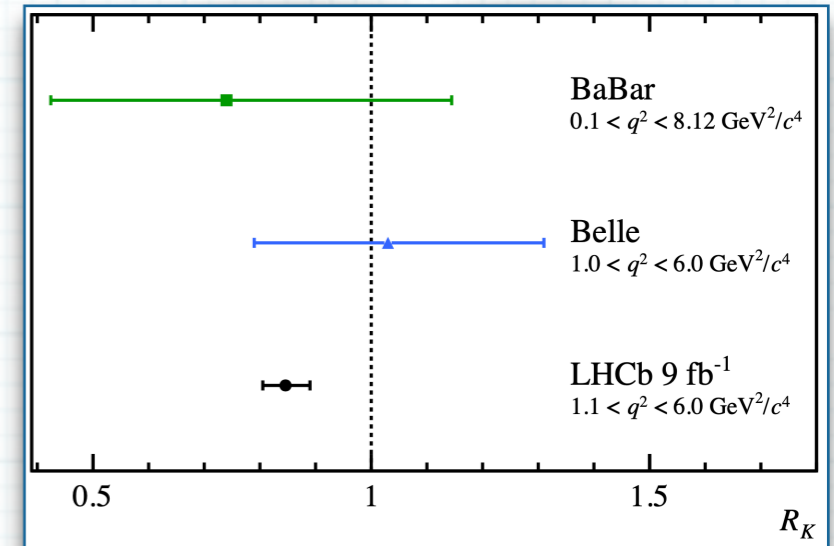
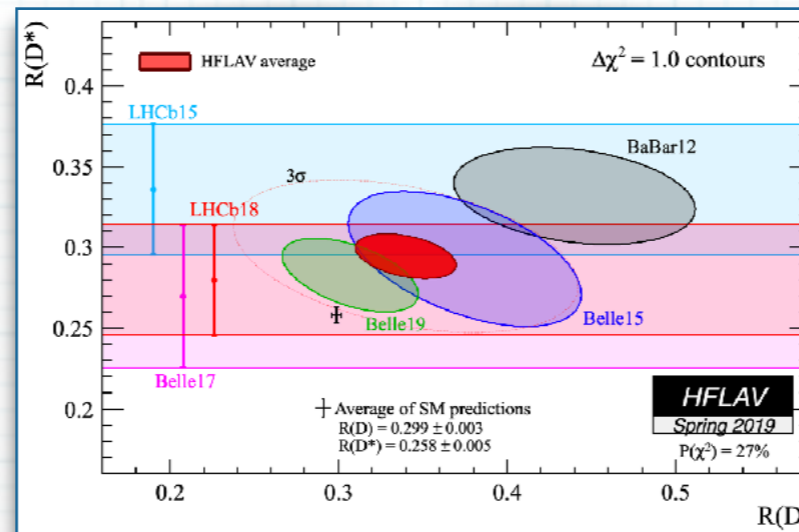
Based on 2101.12069

Violation of Lepton Flavour Universality! New Physics?

- LFU is in tension with recent experimental measurements of semileptonic B-meson decays.

$$R_{D^{(*)}} = \frac{\mathcal{B}(B \rightarrow D^{(*)}\tau\bar{\nu})}{\mathcal{B}(B \rightarrow D^{(*)}\ell\bar{\nu})}$$

$$R_{K^{(*)}} = \frac{\mathcal{B}(B \rightarrow K^{(*)}\mu^+\mu^-)}{\mathcal{B}(B \rightarrow K^{(*)}e^+e^-)}$$



- A TeV-scale charge-2/3 weak-singlet vLQ $U_1 \equiv (\mathbf{3}, \mathbf{1}, 2/3)$ can resolve both $R_{D^{(*)}}$ and $R_{K^{(*)}}$ anomalies simultaneously. It is a color-triplet vector boson with nonzero lepton and baryon numbers.

Bottom-Up Scenarios

- ▶ The interaction Lagrangian

$$\mathcal{L} \supset x_{1ij}^{LL} \bar{Q}^i \gamma_\mu U_1^\mu P_L L^j + x_{1ij}^{RR} \bar{d}_{Ri} \gamma_\mu U_1^\mu P_R \ell_R^j + \text{H.c.}$$

- ▶ x_{1ij}^{LL} and x_{1ij}^{RR} are 3×3 matrices in flavour space. We assume them to be real. Since we are interested in the $R_{D^{(*)}}$ and $R_{K^{(*)}}$ anomalies, we set all components that do not participate directly in these decays to zero.

$R_{D^{(*)}}$ Operators

- ▶ U_1 contribution to the $b \rightarrow c\tau\bar{\nu}$ transition

$$\mathcal{L} \supset -\frac{4G_F}{\sqrt{2}} V_{cb} \left[\left(1 + \mathcal{C}_{V_L}\right) \mathcal{O}_{V_L} + \mathcal{C}_{S_L} \mathcal{O}_{S_L} \right]$$

$$\mathcal{C}_{V_L}^{U_1} = \frac{1}{2\sqrt{2}G_F V_{cb}} \frac{\lambda_{c\nu}^L (\lambda_{b\tau}^L)^*}{M_{U_1}^2}, \quad \mathcal{C}_{S_L}^{U_1} = -\frac{1}{2\sqrt{2}G_F V_{cb}} \frac{2\lambda_{c\nu}^L (\lambda_{b\tau}^R)^*}{M_{U_1}^2}$$

Flavour Ansatz

$$x_1^{LL} = \begin{pmatrix} 0 & 0 & 0 \\ 0 & 0 & \lambda_{23}^L \\ 0 & 0 & \lambda_{33}^L \end{pmatrix}$$

$$x_1^{RR} = \begin{pmatrix} 0 & 0 & 0 \\ 0 & 0 & 0 \\ 0 & 0 & \lambda_{33}^R \end{pmatrix}$$

- ▶ Nonzero \mathcal{C}_{V_L} and \mathcal{C}_{S_L} would also contribute to other observables like $F_L(D^*)$, $P_\tau(D^*)$, etc.

R_{D(*)} Scenarios

- ▶ We construct scenarios with one and two nonzero couplings.

R _{D(*)} scenarios	λ _{cv} ^L	λ _{bτ} ^L	λ _{bτ} ^R
RD1A	λ ₂₃ ^L	V _{cb} [*] λ ₂₃ ^L	—
RD1B	V _{cb} λ ₃₃ ^L	λ ₃₃ ^L	—
RD2A	V _{cs} λ ₂₃ ^L + V _{cb} λ ₃₃ ^L	λ ₃₃ ^L	—
RD2B	V _{cs} λ ₂₃ ^L	—	λ ₃₃ ^R

R_{K(*)} Operators

- ▶ A general Lagrangian for $b \rightarrow s\mu^+\mu^-$ transition

$$\mathcal{L} \supset \frac{4G_F}{\sqrt{2}} V_{tb} V_{ts}^* \sum_{i=9,10,S,P} (\mathcal{C}_i \mathcal{O}_i + \mathcal{C}'_i \mathcal{O}'_i)$$

Flavour Ansatz

$$x_1^{LL} = \begin{pmatrix} 0 & 0 & 0 \\ 0 & \lambda_{22}^L & 0 \\ 0 & \lambda_{32}^L & 0 \end{pmatrix}$$

$$x_1^{RR} = \begin{pmatrix} 0 & 0 & 0 \\ 0 & \lambda_{22}^R & 0 \\ 0 & \lambda_{32}^R & 0 \end{pmatrix}$$

$$\mathcal{C}_9^{U_1} = -\mathcal{C}_{10}^{U_1} = \frac{\pi}{\sqrt{2}G_F V_{tb} V_{ts}^* \alpha} \frac{\lambda_{s\mu}^L (\lambda_{b\mu}^L)^*}{M_{U_1}^2}$$

$$\mathcal{C}_S^{U_1} = -\mathcal{C}_P^{U_1} = \frac{\sqrt{2}\pi}{G_F V_{tb} V_{ts}^* \alpha} \frac{\lambda_{s\mu}^L (\lambda_{b\mu}^R)^*}{M_{U_1}^2}$$

$$\mathcal{C}'_9{}^{U_1} = \mathcal{C}'_{10}{}^{U_1} = \frac{\pi}{\sqrt{2}G_F V_{tb} V_{ts}^* \alpha} \frac{\lambda_{s\mu}^R (\lambda_{b\mu}^{R*})}{M_{U_1}^2}$$

$$\mathcal{C}'_S{}^{U_1} = \mathcal{C}'_P{}^{U_1} = \frac{\sqrt{2}\pi}{G_F V_{tb} V_{ts}^* \alpha} \frac{\lambda_{s\mu}^R (\lambda_{b\mu}^{L*})}{M_{U_1}^2}$$

$R_{K^{(*)}}$ Scenarios

- ▶ We construct scenarios with one and two nonzero couplings.

$R_{K^{(*)}}$ scenarios	$\lambda_{s\mu}^L$	$\lambda_{b\mu}^L$	$\lambda_{s\mu}^R$	$\lambda_{b\mu}^R$
RK1A	$V_{cs}^* \lambda_{22}^L$	$V_{cb}^* \lambda_{22}^L$	—	—
RK1B	$V_{ts}^* \lambda_{32}^L$	$V_{tb}^* \lambda_{32}^L$	—	—
RK1C	—	—	$V_{cs} \lambda_{22}^R$	$V_{cb} \lambda_{22}^R$
RK1D	—	—	$V_{ts} \lambda_{32}^R$	$V_{tb} \lambda_{32}^R$
RK2A	λ_{22}^L	λ_{32}^L	—	—
RK2B	λ_{22}^L	—	—	λ_{32}^R
RK2C	—	λ_{32}^L	λ_{22}^R	—
RK2D	—	—	λ_{22}^R	λ_{32}^R

Different Scenarios, Different Signatures

- ▶ In these scenarios, the production modes and the dominant decay modes of U_1 would vary. Hence, an U_1 might lead to different signatures in different scenarios.

$$pp \rightarrow \left\{ \begin{array}{l} U_1 U_1 \rightarrow s\mu s\mu \equiv \mu\mu + 2j \\ U_1 U_1 \rightarrow s\mu c\nu \equiv \mu + \cancel{E}_T + 2j \\ U_1 U_1 \rightarrow c\nu c\nu \equiv \cancel{E}_T + 2j \end{array} \right\}$$

λ_{22}^L (RK1A)

$$pp \rightarrow \left\{ \begin{array}{l} U_1 U_1 \rightarrow b\mu b\mu \equiv \mu\mu + 2j \\ U_1 U_1 \rightarrow b\mu t\nu \equiv \mu + \cancel{E}_T + j_t + j \\ U_1 U_1 \rightarrow t\nu t\nu \equiv \cancel{E}_T + 2j_t \end{array} \right\}$$

λ_{32}^L (RK1B)

Pair Production

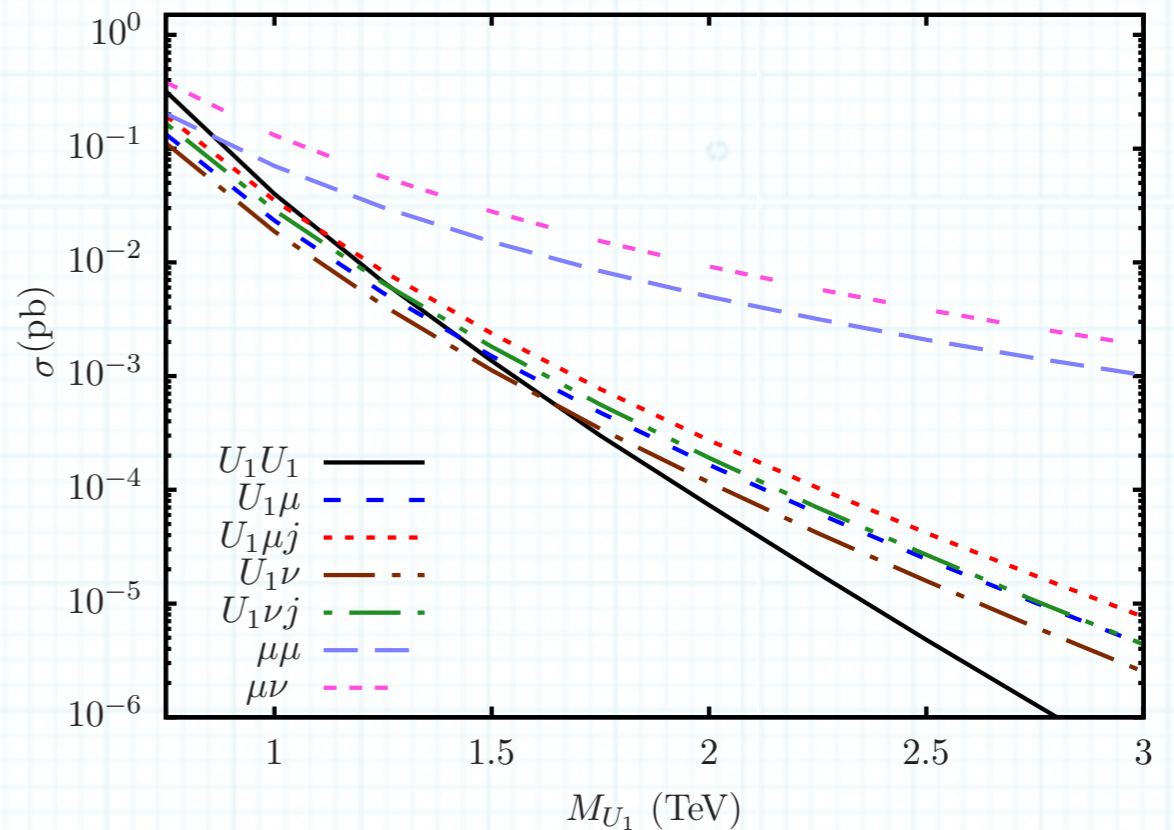
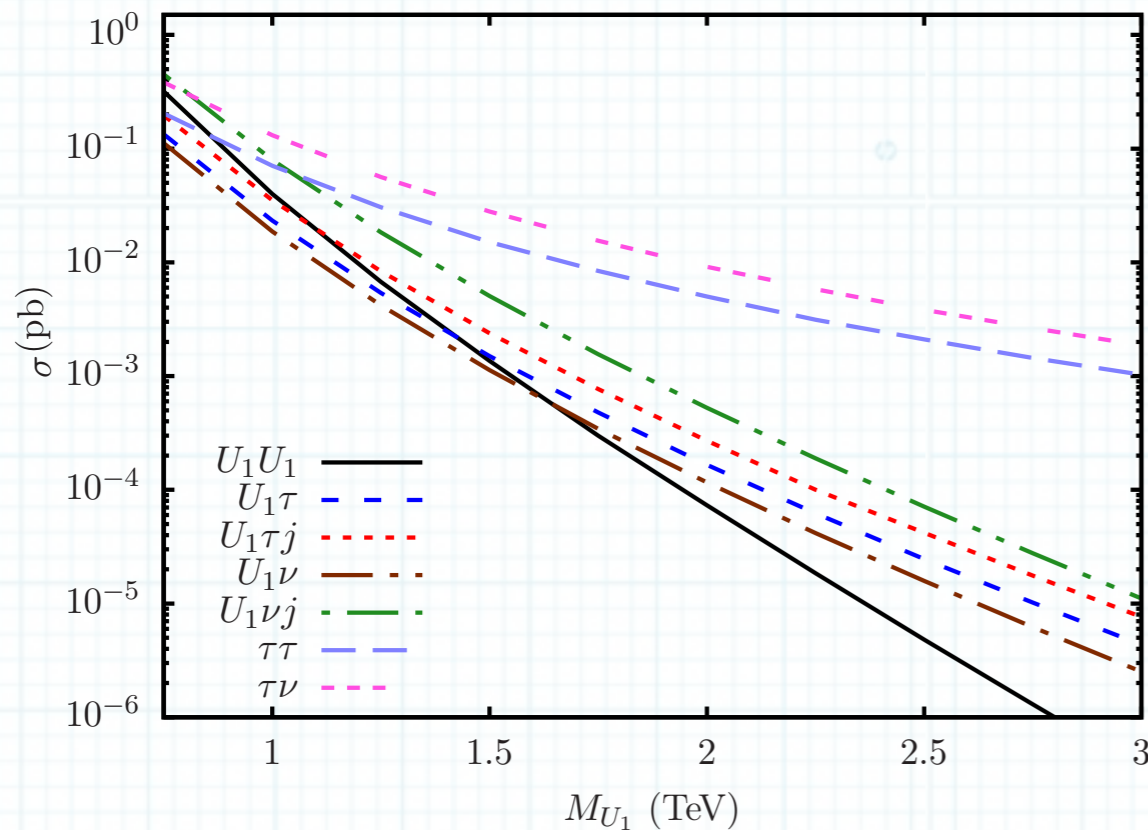
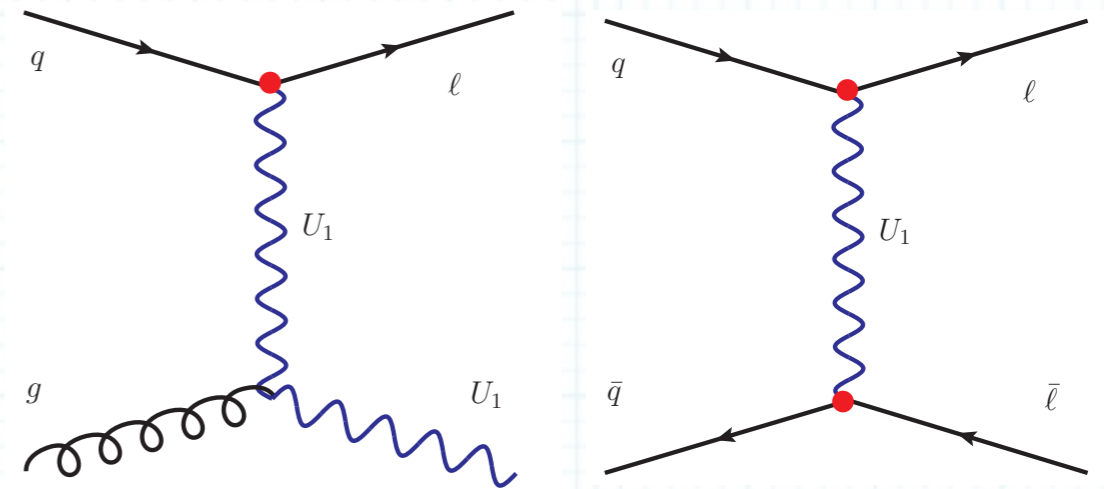
- Possible final states. A simple parametrisation to show the relative strengths.

Nonzero couplings	Signatures					
	$\tau\tau + 2j$	$\tau + \cancel{E}_T + 2j$	$\cancel{E}_T + 2j$	$\tau + \cancel{E}_T + j_t + j$	$\cancel{E}_T + 2j_t$	$\cancel{E}_T + j_t + j$
λ_{23}^L (Scenario RD1A)	0.25	0.50	0.25	—	—	—
λ_{33}^L (Scenario RD1B)	0.25	—	—	0.50	0.25	—
λ_{33}^R	1.00	—	—	—	—	—
$\lambda_{23}^L, \lambda_{33}^L$ (Scenario RD2A)	0.25	ξ	ξ^2	$\frac{1}{2} - \xi$	$(\frac{1}{2} - \xi)^2$	$2\xi(\frac{1}{2} - \xi)$
$\lambda_{23}^L, \lambda_{33}^R$ (Scenario RD2B)	$(\frac{1}{2} + \xi)^2$	$2(\frac{1}{4} - \xi^2)$	$(\frac{1}{2} - \xi)^2$	—	—	—
	$\mu\mu + 2j$	$\mu + \cancel{E}_T + 2j$	$\cancel{E}_T + 2j$	$\mu + \cancel{E}_T + j_t + j$	$\cancel{E}_T + 2j_t$	$\cancel{E}_T + j_t + j$
λ_{22}^L (Scenario RK1A)	0.25	0.50	0.25	—	—	—
λ_{32}^L (Scenario RK1B)	0.25	—	—	0.50	0.25	—
λ_{22}^R (Scenario RK1C)	1.00	—	—	—	—	—
λ_{32}^R (Scenario RK1D)	1.00	—	—	—	—	—
$\lambda_{22}^L, \lambda_{32}^L$ (Scenario RK2A)	0.25	ξ	ξ^2	$\frac{1}{2} - \xi$	$(\frac{1}{2} - \xi)^2$	$2\xi(\frac{1}{2} - \xi)$
$\lambda_{22}^L, \lambda_{32}^R$ (Scenario RK2B)	$(\frac{1}{2} + \xi)^2$	$2(\frac{1}{4} - \xi^2)$	$(\frac{1}{2} - \xi)^2$	—	—	—
$\lambda_{22}^R, \lambda_{32}^L$ (Scenario RK2C)	$(\frac{1}{2} + \xi)^2$	—	—	$2(\frac{1}{4} - \xi^2)$	$(\frac{1}{2} - \xi)^2$	—
$\lambda_{22}^R, \lambda_{32}^R$ (Scenario RK2D)	1.00	—	—	—	—	—

ξ is a free parameter

Single and Non-Resonant Productions

- ▶ λ -dependent single productions and t -channel LQ exchange.
- ▶ If λ is not small and/or the U_1 is heavy, they are the dominant processes.
- ▶ Non-resonant production does not depend on branching ratios.

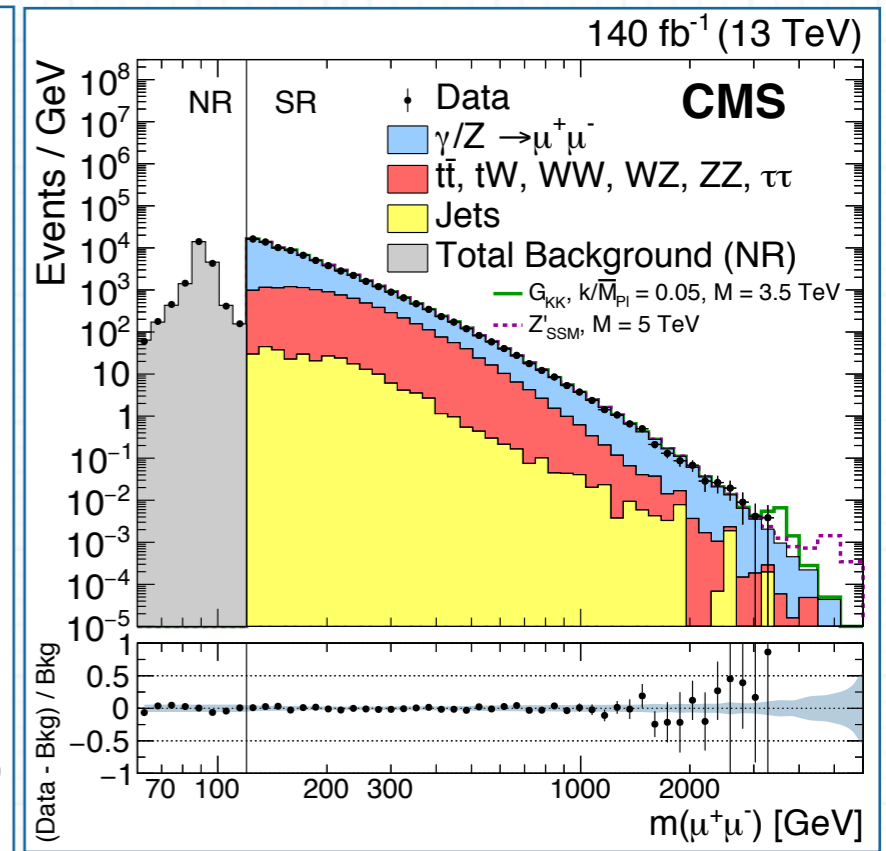
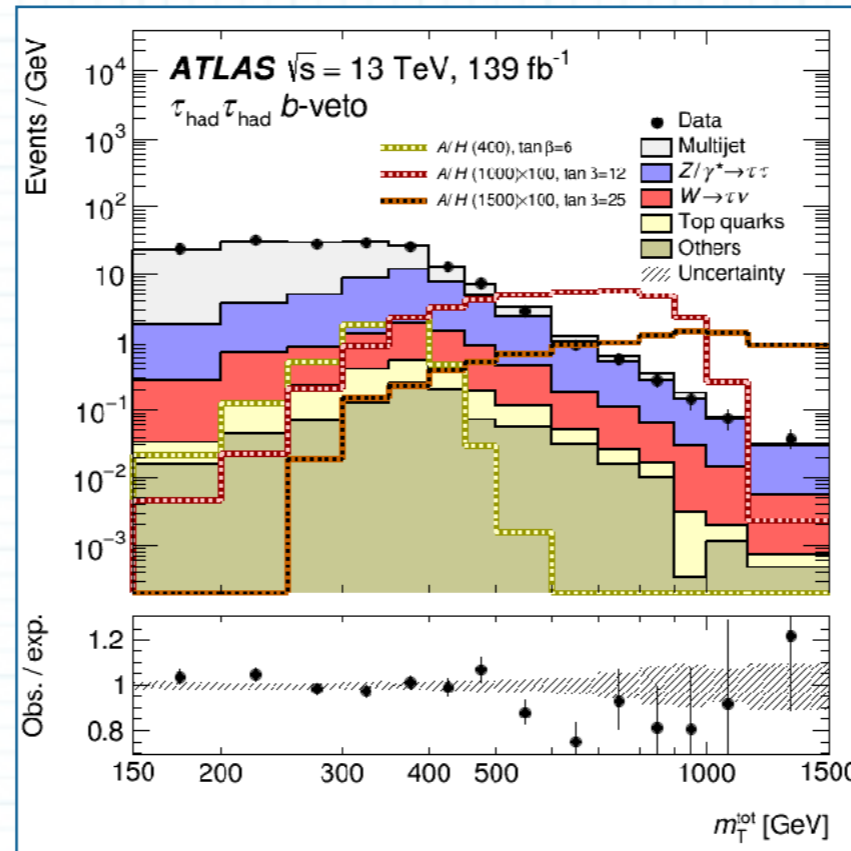


ATLAS $\tau\tau$ (139 fb^{-1}) and CMS $\mu\mu$ (140 fb^{-1}) Resonance Searches

- ▶ All three production modes would lead to $\ell\ell + \text{jets}$ final states.
- ▶ The signal to the dilepton searches would be a combination of these three processes + the interference of t -channel process with the $SMpp \rightarrow Z/\gamma \rightarrow \ell\ell$ process.
- ▶ The interference is destructive, leading to a reduction of events.

2002.12223

2103.02708



Mass (TeV)	Pair production			Single production			t -channel LQ			Interference		
	σ^p	ϵ^p	\mathcal{N}^p	σ^s	ϵ^s	\mathcal{N}^s	σ^{nr4}	ϵ^{nr4}	\mathcal{N}^{nr4}	σ^{nr2}	ϵ^{nr2}	\mathcal{N}^{nr2}

Contribution to $\tau\tau$ signal [82]

$\lambda_{23}^L = 1$ (Scenario RD1A)												
1.0	40.87	2.33	8.59	58.80	3.30	35.07	70.57	7.22	183.33	-232.63	3.17	-266.21
1.5	1.39	1.50	0.19	3.91	2.74	1.93	14.94	7.00	37.77	-104.31	3.34	-125.62
2.0	0.08	1.01	0.01	0.44	2.50	0.20	5.04	7.25	13.19	-58.79	3.28	-69.57
$\lambda_{33}^L = 1$ (Scenario RD1B)												
1.0	35.67	1.69	5.43	29.00	2.57	13.46	20.20	6.21	45.26	-75.02	3.08	-83.41
1.5	1.17	1.09	0.11	1.72	2.16	0.67	4.31	6.22	9.68	-33.62	2.88	-33.01
2.0	0.06	0.81	0.00	0.17	1.98	0.06	1.39	6.27	3.15	-18.97	2.88	-19.71

A χ^2 Test

- ▶ For each distribution, we define the test statistic as

$$\chi^2 = \sum_i^{\text{bins}} \left(\frac{\mathcal{N}_T^i(M_{U_1}, \lambda) - \mathcal{N}_D^i}{\Delta \mathcal{N}^i} \right)^2$$

- ▶ $\mathcal{N}_T^i(M_{U_1}, \lambda)$ = theory events and \mathcal{N}_D^i = the number of observed events in the i^{th} bin.

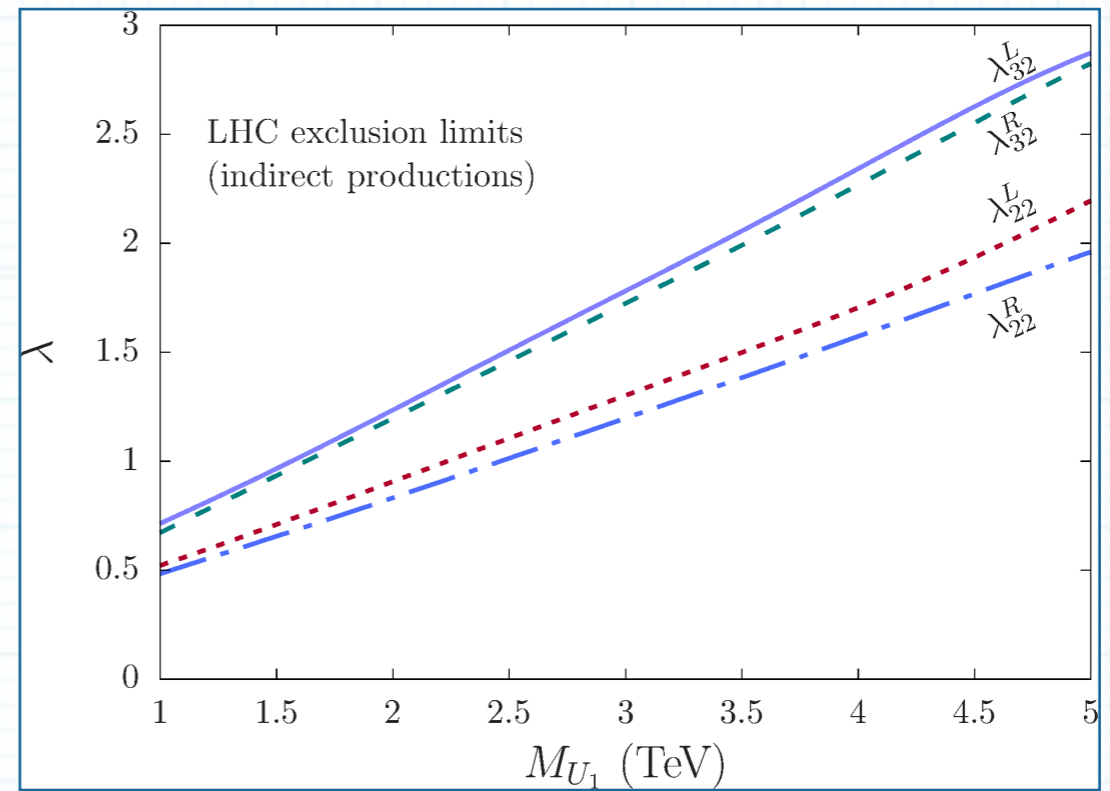
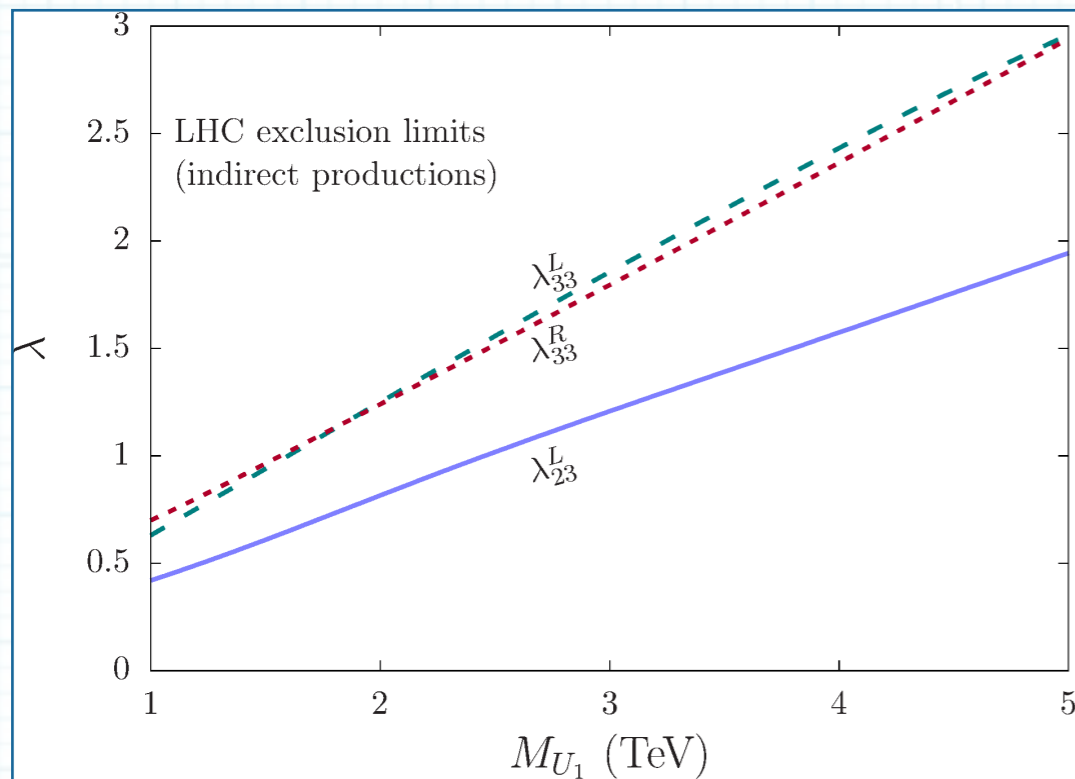
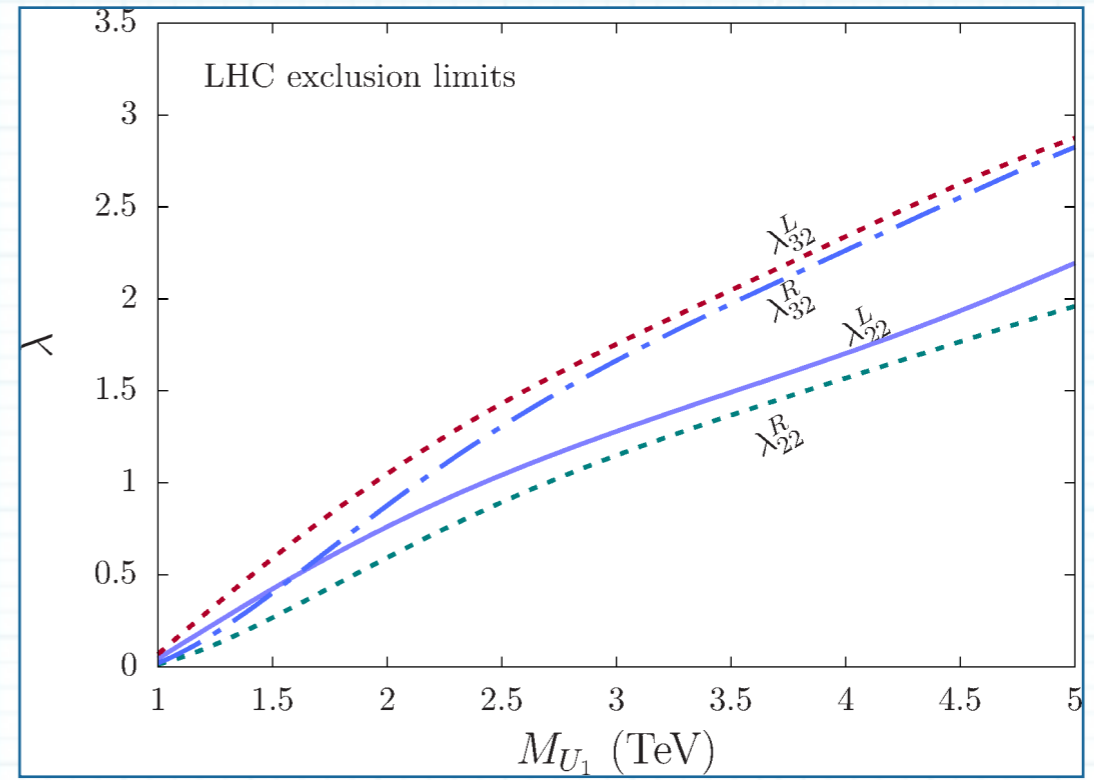
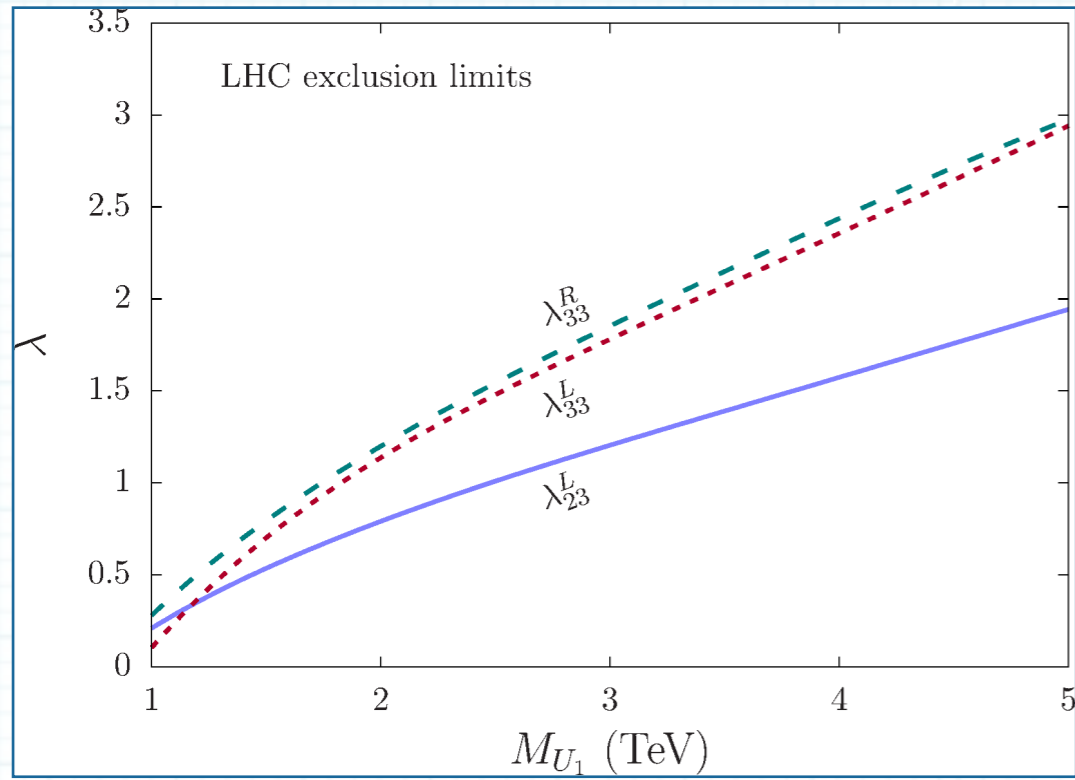
$$\mathcal{N}_T^i(M_{U_1}, \lambda) = [\mathcal{N}^p(M_{U_1}, \lambda) + \mathcal{N}^s(M_{U_1}, \lambda) + \mathcal{N}^{nr}(M_{U_1}, \lambda)] + \mathcal{N}_{\text{SM}}^i.$$

- ▶ For the error $\Delta \mathcal{N}^i$, we use

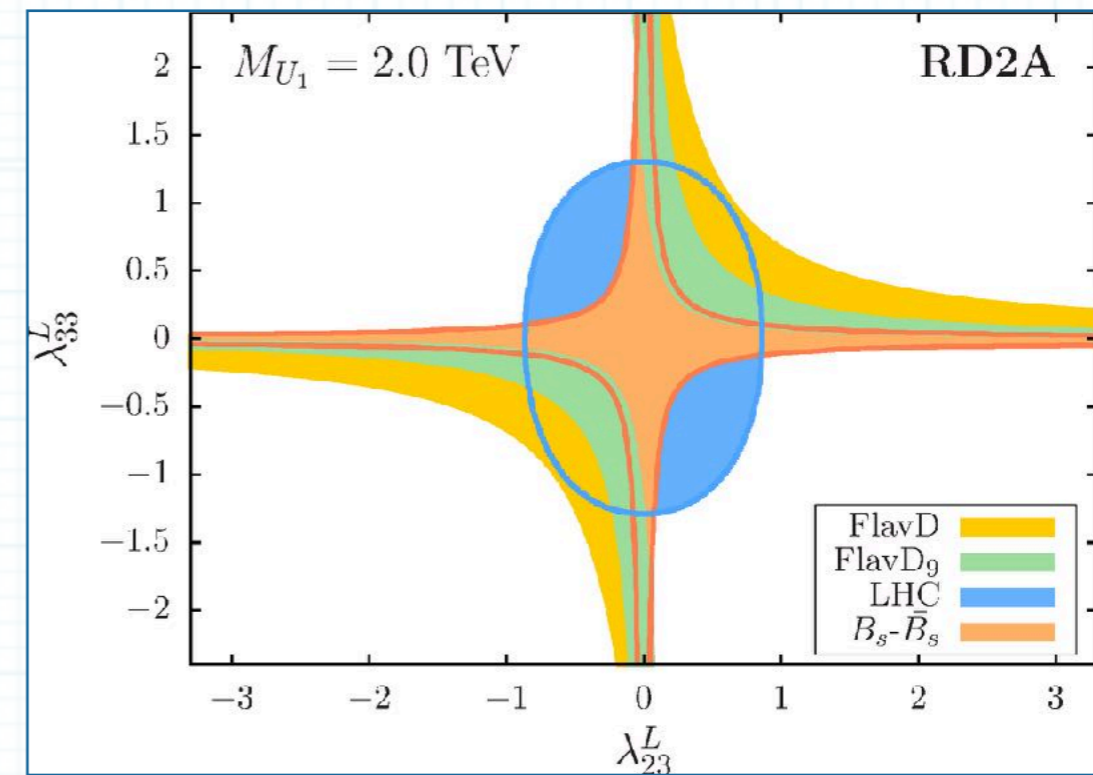
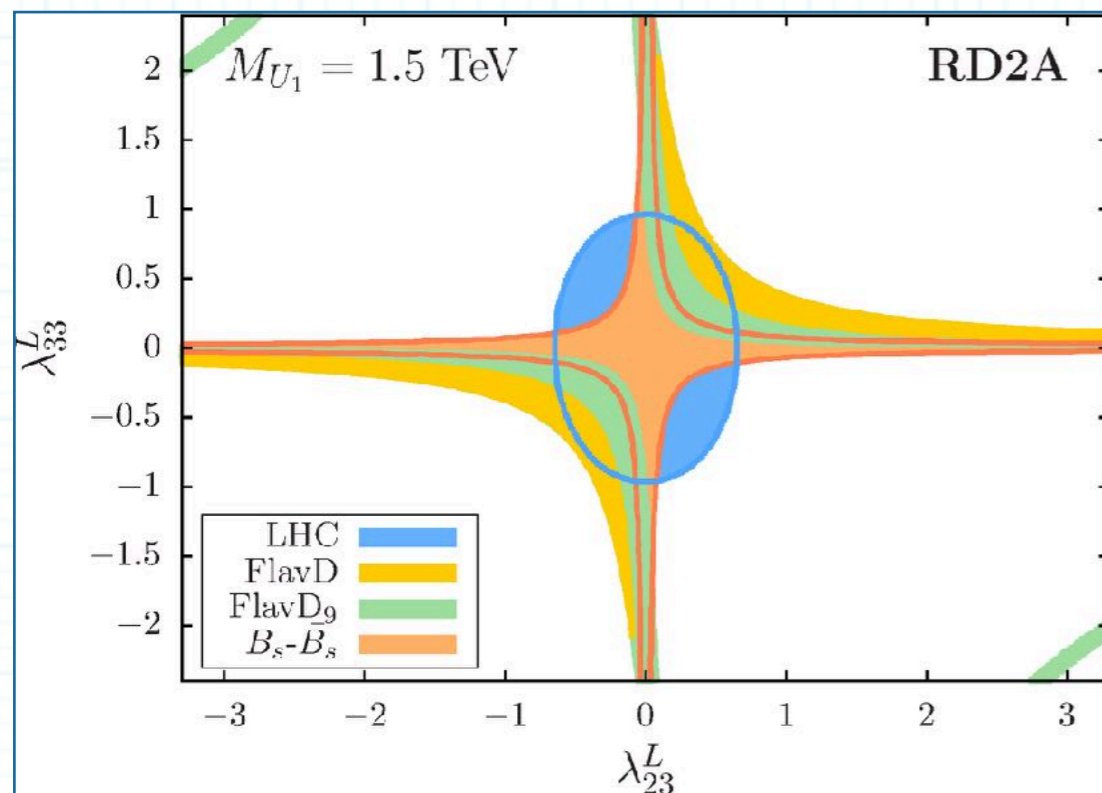
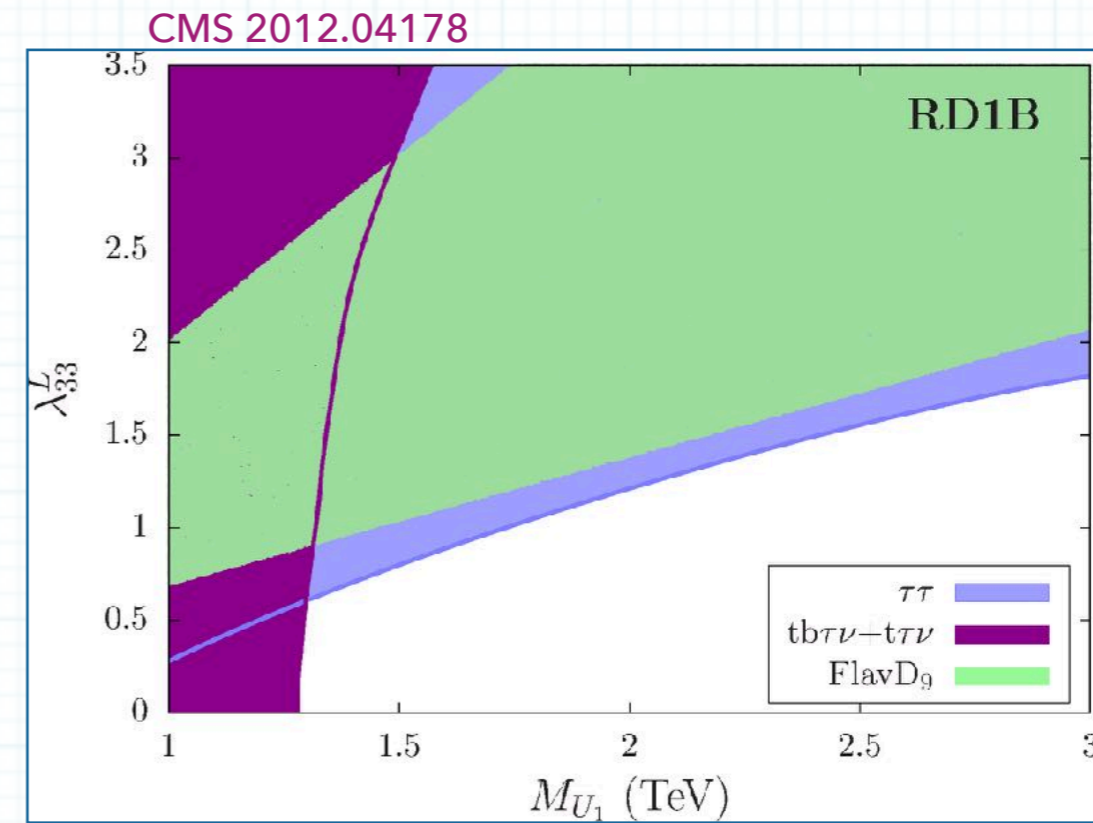
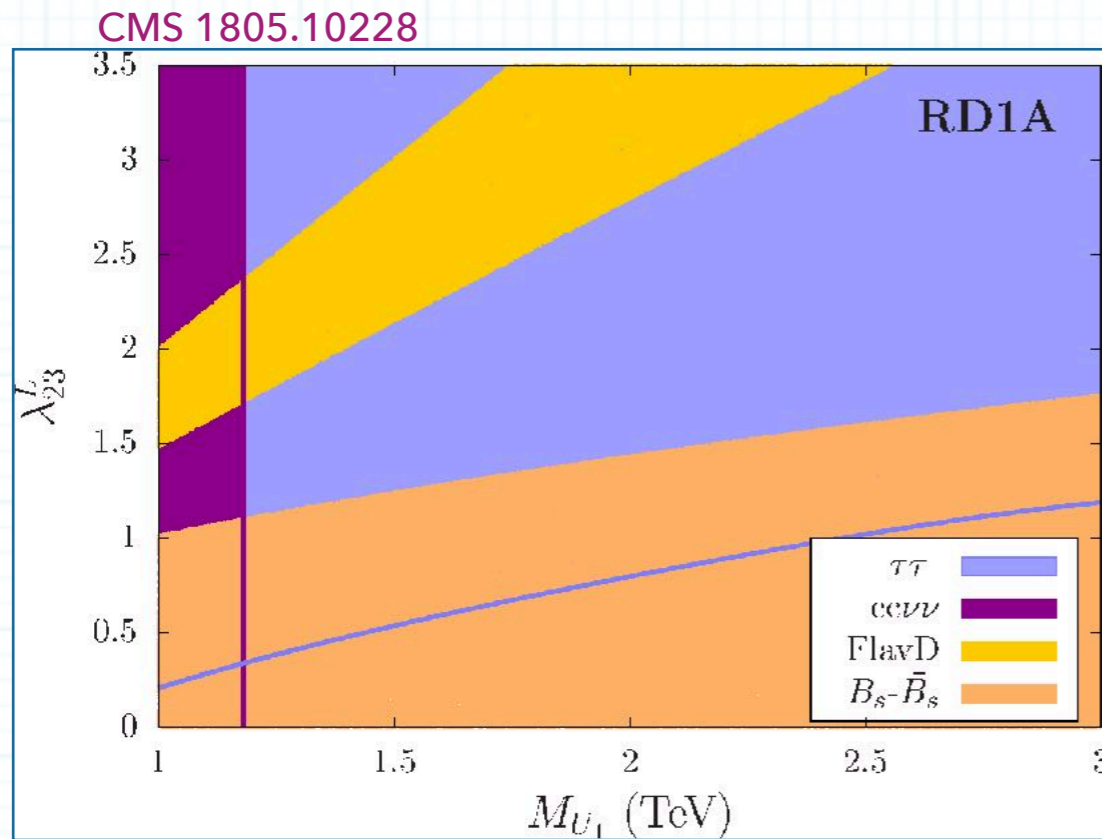
$$\Delta \mathcal{N}^i = \sqrt{(\Delta \mathcal{N}_{\text{stat}}^i)^2 + (\Delta \mathcal{N}_{\text{syst}}^i)^2}$$

where $\Delta \mathcal{N}_{\text{stat}}^i = \sqrt{\mathcal{N}_D^i}$ and we assume a uniform **10%** systematic error

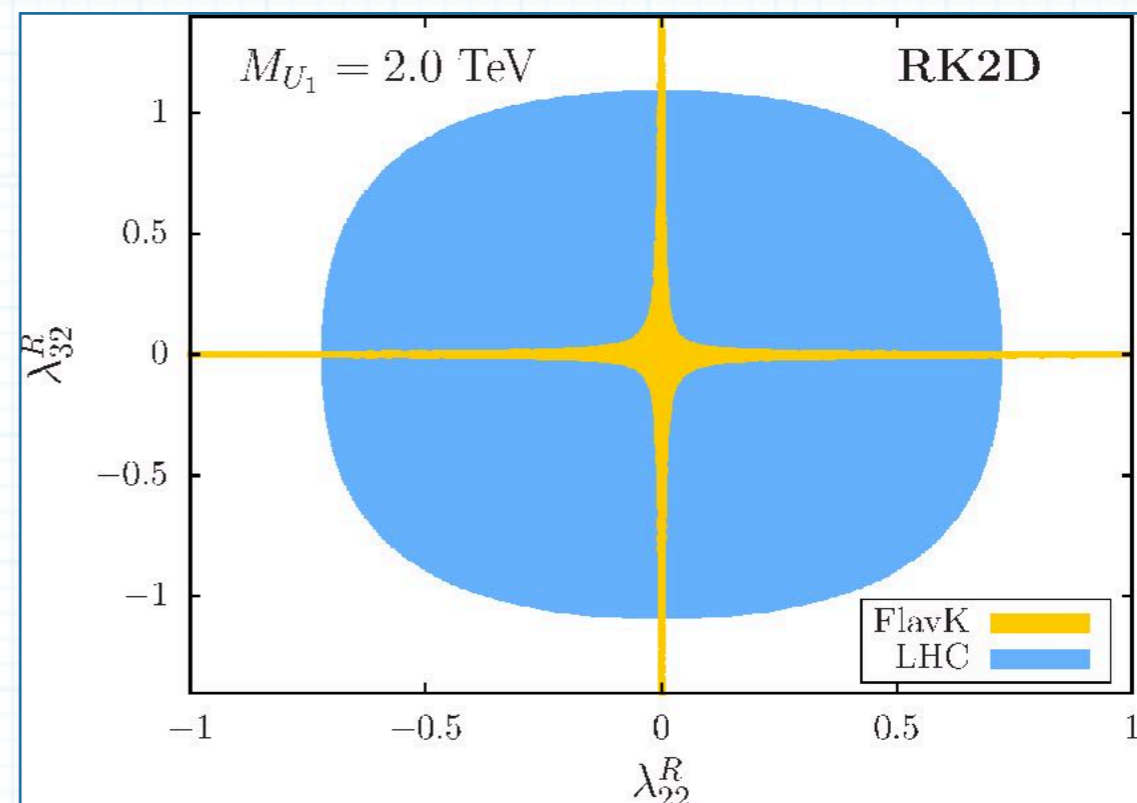
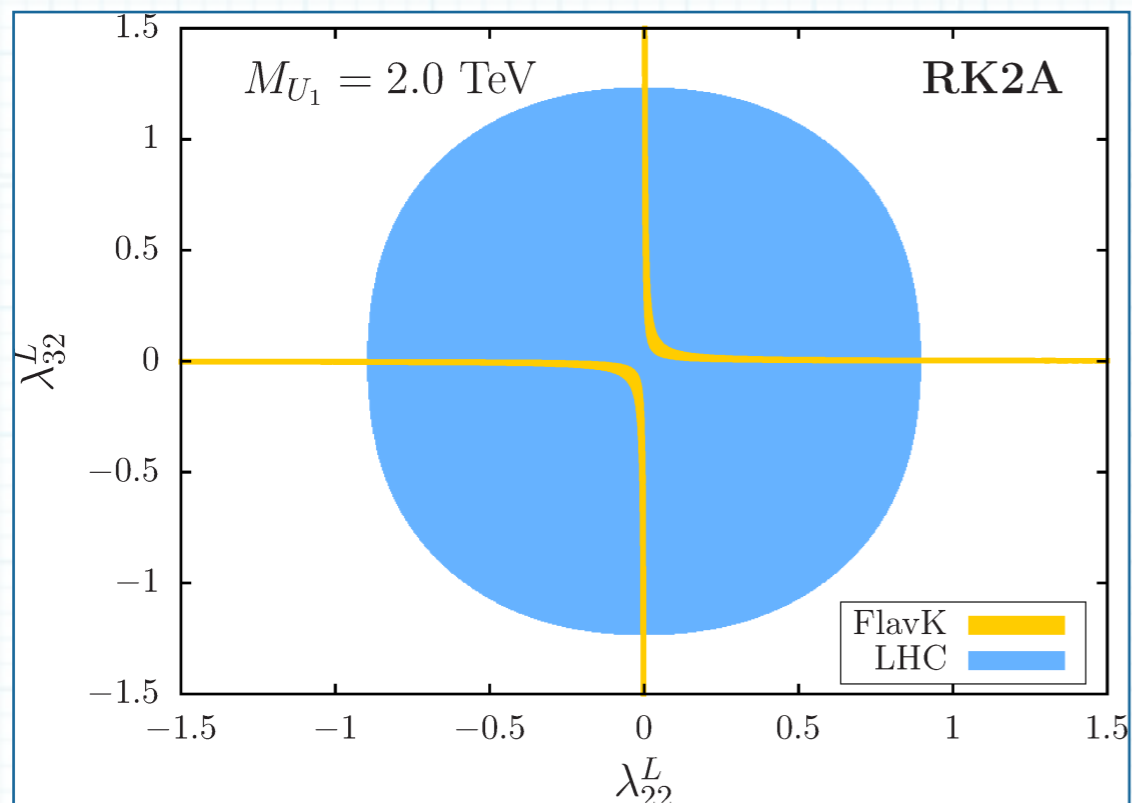
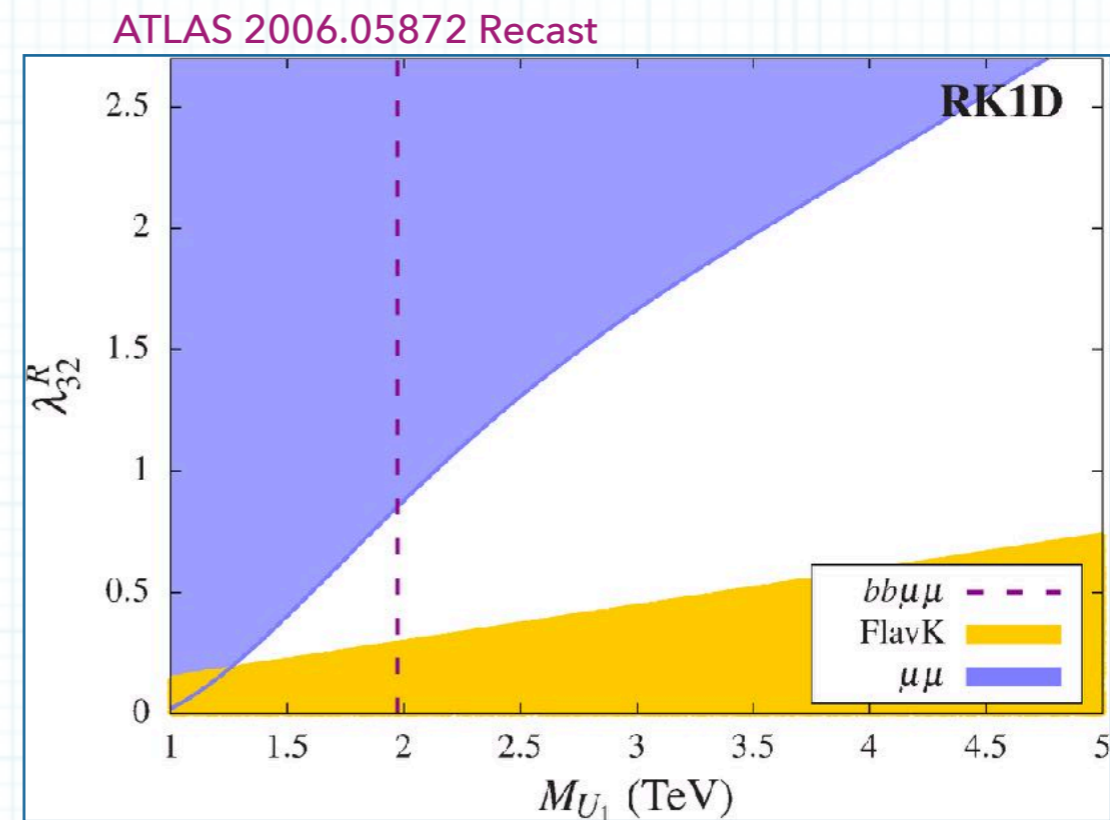
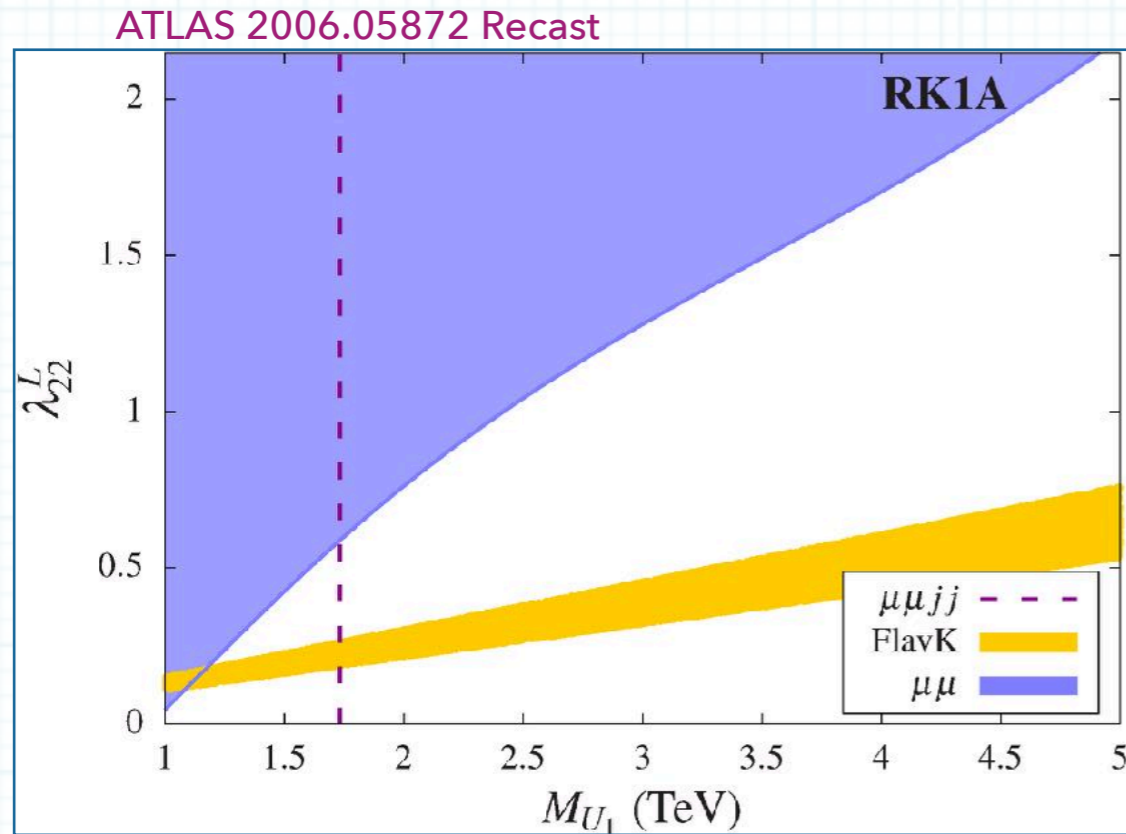
- ▶ In every scenario, for some benchmark masses $M_{U_1} = M_{U_1}^b$, we compute the minimum of χ^2 by varying the couplings. In one-coupling scenarios, we obtain the **1 σ** and **2 σ** CL upper limit on the coupling at $M_{U_1}^b$ from the values of λ for which $\Delta \chi^2(M_{U_1}^b, \lambda) = \chi^2(M_{U_1}^b, \lambda) - \chi_{\text{min}}^2(M_{U_1}^b)$ equals **1** and **4**, respectively.
- ▶ The limits on multi-coupling scenarios can be obtained similarly.



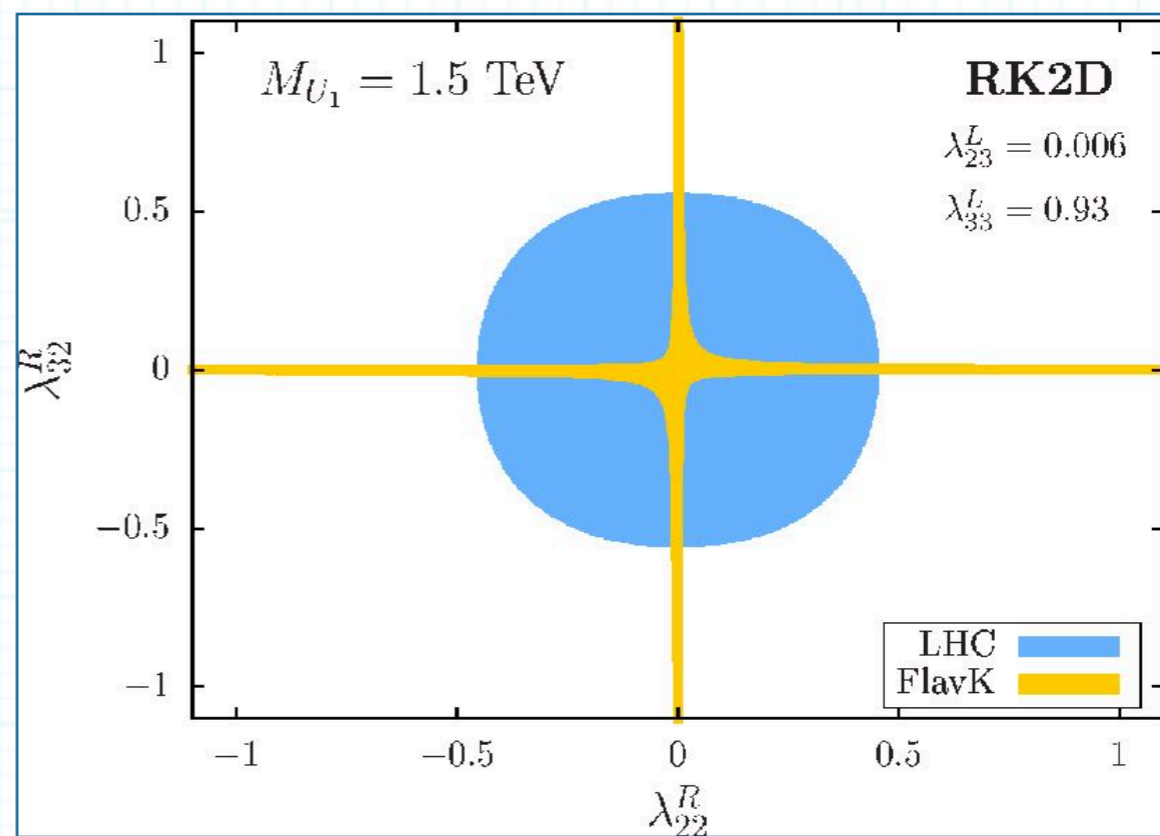
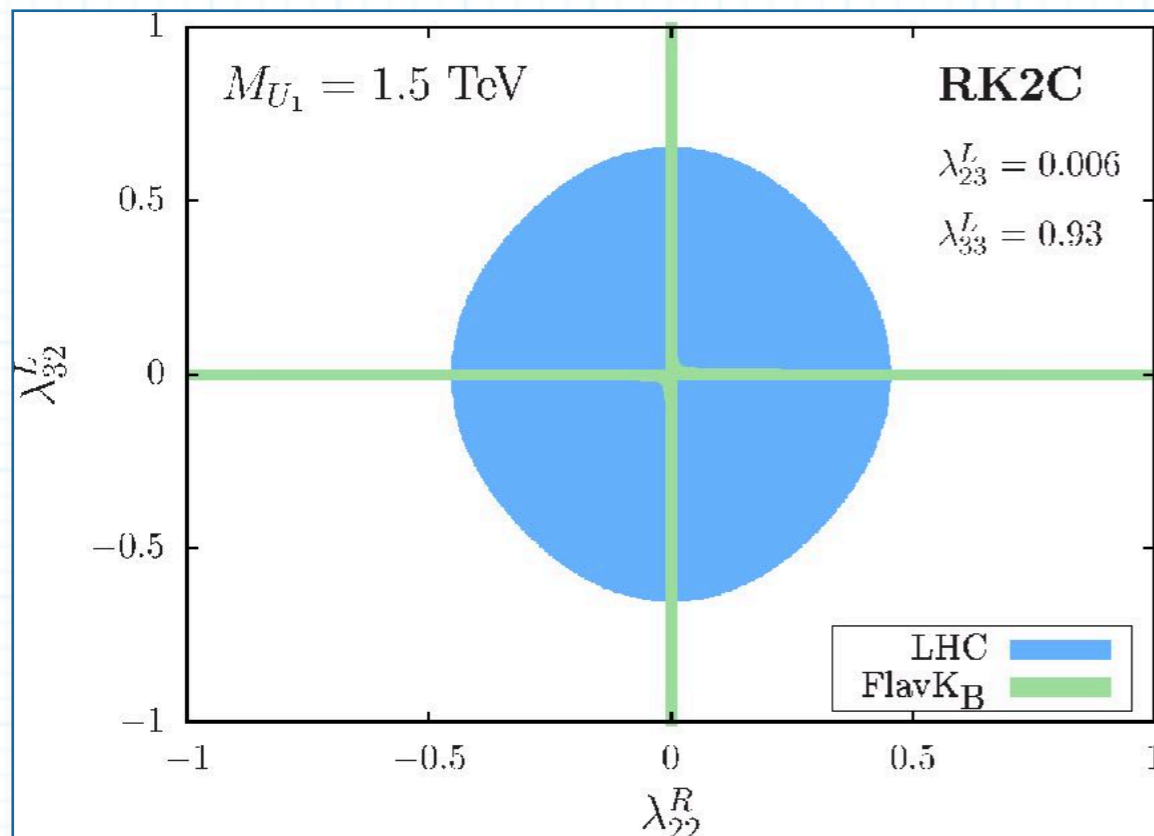
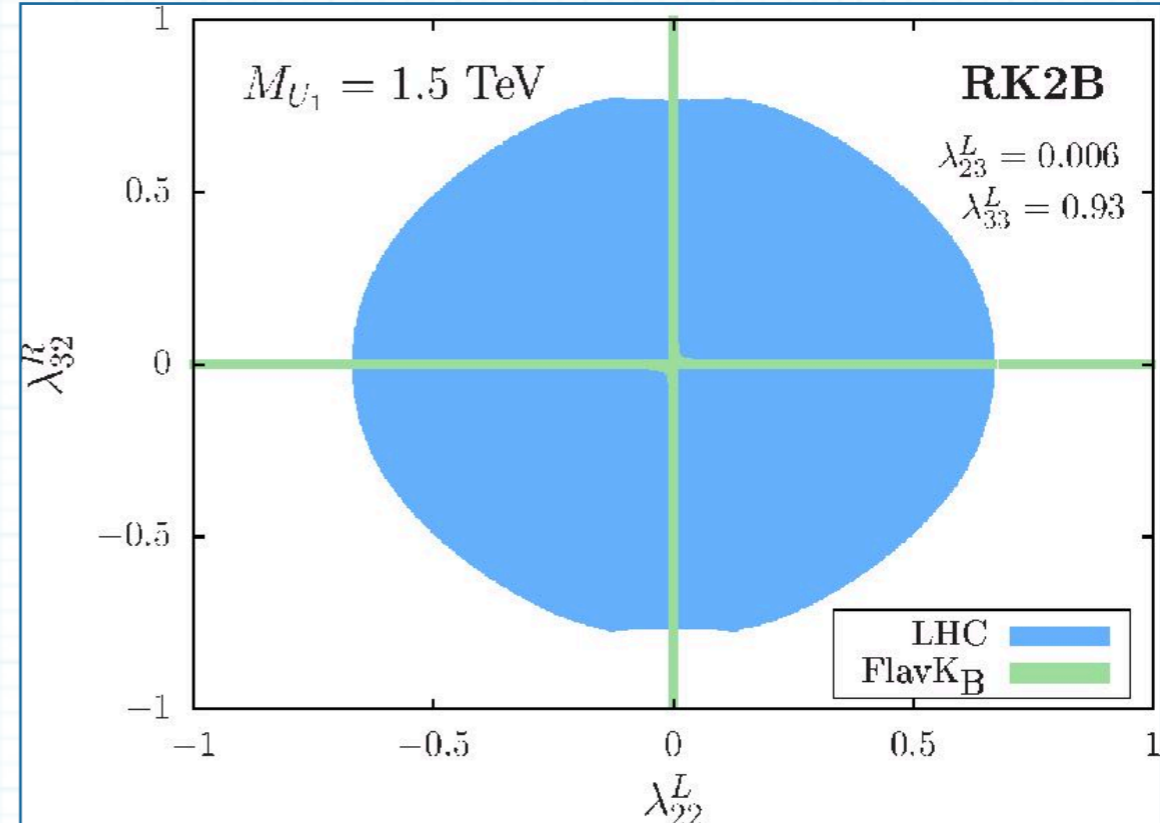
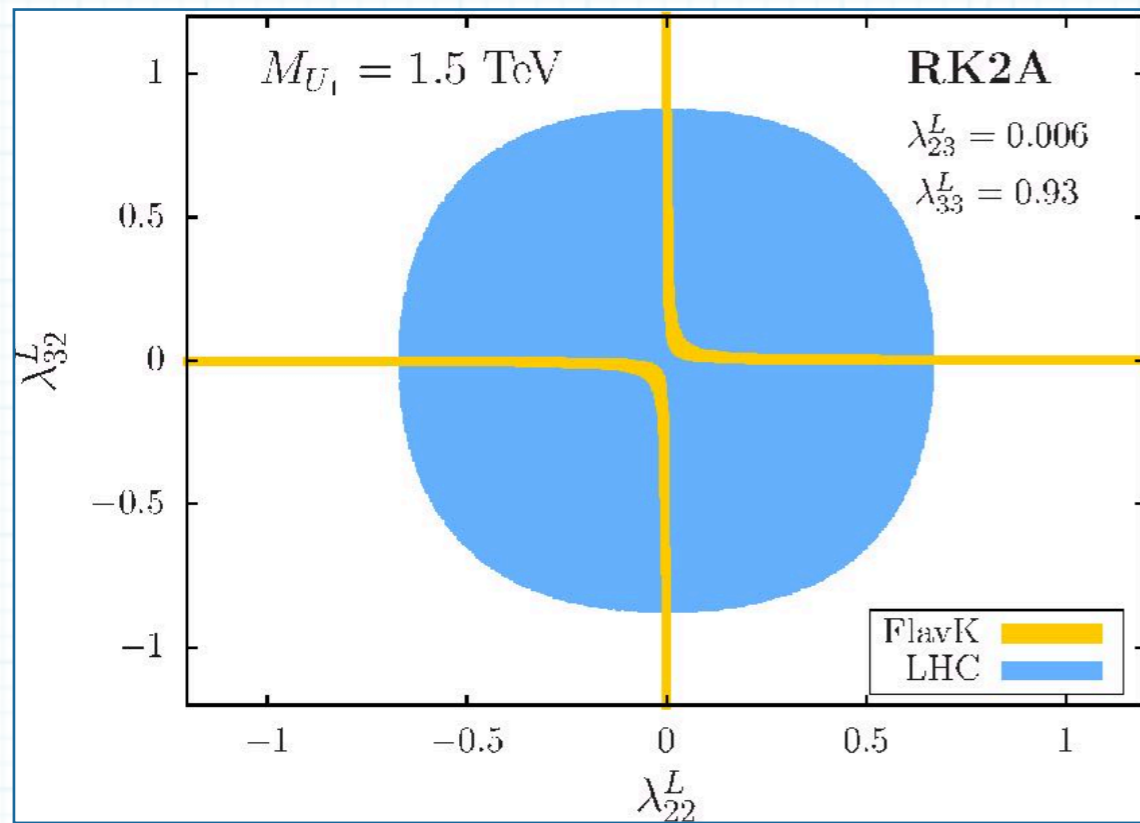
The $R_{D^{(*)}}$ Scenarios Are Severely Constrained



Recast of ATLAS Scalar LQ Search Data Rules out U_1 Below ~ 2 TeV



A 1.5 TeV U_1 Can Explain Both the Anomalies



Thank you

PHENO 2021

LHC LIMITS ON THE B-ANOMALIES MOTIVATED U_1 LEPTOQUARK MODELS

SUBHADIP MITRA (IIIT HYDERABAD)

May 25, 2021

In collaboration with Arvind Bhaskar, Diganta Das, Tanumoy Mandal, & Cyrin Neeraj

Based on 2101.12069